Original

Nebebe Mekonen, M.; Bohlen, J.; Steglich, D.; Mosler, J.:

Numerical simulation of forming limit test for AZ31 at 200°C

Key Engineering Materials, Sheet Metal 2011 (2011)
Trans Tech Publications

DOI: 10.4028/www.scientific.net/KEM.473.468

Key Engineering Materials
ISSN: 1662-9795, Vol. 473, pp 468-473
doi:10.4028/www.scientific.net/KEM.473.468
© 2011 Trans Tech Publications, Switzerland
Online: 2011-03-28

Numerical simulation of forming limit test for AZ31 at 200°C

M. Nebebe[a], J. Bohlen[b], D. Steglich[c], J. Mosler[d]

Helmholtz-Zentrum Geesthacht, Institute of Materials Research, D-21502 Geesthacht, Germany

[a] Mintesnot.Nebebe@hzg.de, [b]Jan.Bohlen@hzg.de, [c]Dirk.Steglich@hzg.de, [d]Joern.Mosler@hzg.de

Keywords: Mg alloy, Constitutive model, Sheet forming limits

Abstract. This work is concerned with numerical analyses of the forming behavior of magnesium at elevated temperature. For that purpose, a thermodynamically consistent, rate-dependent, finite-strain elasto-plastic constitutive model is presented. This model captures the stress differential effect as well as the anisotropy of magnesium. Furthermore, the change in shape of the yield locus (distortional hardening) is also taken into account. This constitutive law, together with its parameter calibration based on uni-axial tensile tests, is finally combined with the localization criterion originally proposed by Marciniak and Kuczynski and applied to the simulation of forming limit test. Comparisons to experiments show the excellent predictive capabilities of the model.

Introduction

Although its high strength-to-weight ratio makes magnesium a very attractive material for light weight structures, its pronounced anisotropy, the compression-tension asymmetry as well as its relatively poor formability, particularly at room temperature, narrow its range of application significantly down, cf. [1,2]. Therefore, recent research is focused on the mechanical behavior of magnesium at elevated temperatures. According to [3,4,5], reasonable formability can be achieved at such conditions. More precisely, the aforementioned studies indicate sufficient formability is observed for temperatures varying between 150°C and 250°C.

Since the sheet forming experiments at elevated temperatures are rather expensive, the accompanying numerical investigations seem to be promising. For that purpose, the elasto-plastic constitutive model as presented in [6] is adopted. This model is capable of capturing the aforementioned properties of magnesium sheets, such as the material anisotropy and the compression-tension asymmetry. For defining the forming limit, the model is combined with a localization criterion, cf. [7,8,9,10]. Within the present paper, the frequently applied and well established approach advocated by Marciniak and Kuczynski is chosen, see [7].

Clearly, for applying a certain constitutive model to the analysis of the forming behavior, its material parameters have to be calibrated first. For that purpose, a constrained optimization scheme based on the genetic algorithm as described in Section 2 of [11] is employed. The respective mechanical properties, such as the stress-strain response necessary for this calibration have been obtained from the uni-axial tensile test results presented in [12,6]. Numerical simulations based on the computed material parameters show that the proposed model captures the forming behavior of magnesium at elevated temperatures very realistically.

Constitutive model and localization criterion

This section presents a thermodynamically consistent hyperelastic-plastic constitutive model incorporating isotropic-distortional hardening as well as a strain rate effect. It is based on a yield function proposed by Cazacu & Barlat [13] (CaBa2004); see also [6]. This yield function allows to describe the well known stress differential effect as well as an initial anisotropy. However and by way of contrast, this yield function is re-written here in tensor notation. For that purpose 4th-order transformation tensors have to be introduced. Even more importantly and different to the original work in [13], such tensors are not constant here, but evolve according to suitable evolution equations. By doing so, a distortional hardening effect can be taken into account (change in shape of the yield locus).

By introducing the modified invariants

$$\mathrm{J}_2^{\mathrm{o}} = \frac{1}{2}\mathrm{tr}(\overline{\boldsymbol{\Sigma}}_{\mathbf{1}} \cdot \overline{\boldsymbol{\Sigma}}_{\mathbf{1}}) \quad \text{and} \quad \mathrm{J}_3^{\mathrm{o}} = \frac{1}{3}\mathrm{tr}(\overline{\boldsymbol{\Sigma}}_{\mathbf{2}} \cdot \overline{\boldsymbol{\Sigma}}_{\mathbf{2}} \cdot \overline{\boldsymbol{\Sigma}}_{\mathbf{2}}), \tag{1}$$

with $\overline{\boldsymbol{\Sigma}}_i = \mathbb{H}_i : \boldsymbol{\Sigma}$ being the modified stress tensors obtained from a linear transformation of the stress tensor $\boldsymbol{\Sigma}$ by the transformation tensors $\mathbb{H}_i$ for $i = 1; 2$, the yield function CaBa2004 can be re-written as

$$f = \mathrm{J}_2^{\mathrm{o}\,3/2} - \mathrm{J}_3^{\mathrm{o}} - h, \tag{2}$$

where h denotes the stress-like isotropic hardening variable.

The strain rate effect is incorporated into the model by the Cowper & Symonds type power law cf. [14], i.e.,

$$\Sigma_{\mathrm{y}}^{\mathrm{ref}} = \; A\,(1 - \exp(B\,\bar{\boldsymbol{\varepsilon}}^{\mathrm{p}})) + C \quad \text{and} \quad \Sigma_{\mathrm{y}} = \; \Sigma_{\mathrm{y}}^{\mathrm{ref}} \left(\frac{\dot{\bar{\boldsymbol{\varepsilon}}}^{\mathrm{p}}}{F\;\dot{\bar{\boldsymbol{\varepsilon}}}^{\mathrm{p}}{}_{\mathrm{ref}}} \right)^{\mathrm{n}}. \tag{3}$$

Here, $\Sigma_{\mathrm{y}}^{\mathrm{ref}}$ is the yield stress at a certain reference strain rate $\dot{\bar{\boldsymbol{\varepsilon}}}^{\mathrm{p}}{}_{\mathrm{ref}}$ and A, B, C, F and n are additional model constants determined based on suitable experimental results. For allowing a change in shape of the yield locus, the distortional tensors (linear transformation) $\mathbb{H}_i$ are assumed to depend on the equivalent plastic strain $\bar{\varepsilon}^{\mathrm{p}}$, i.e.,

$$\mathbb{H}_i = \mathbb{H}_i(\bar{\varepsilon}^{\mathrm{p}}). \tag{4}$$

To ensure thermodynamic consistency of the constitutive model, both hardening models (isotropic as well as distortional), are derived from a Helmholtz energy functional. For guaranteeing the fulfillment of the second law of thermodynamics, evolution equation 4 is chosen such that the resulting dissipation is non-negative. This constraint will also be considered within the model parameter identification.

In order to predict forming limit strains, the well established Marciniak & Kuczynski (MK) localization criterion has been implemented, cf. [10]; see also [15,16,17]. Without going too much into detail, the MK method assumes the existence of an inhomogeneity in the otherwise homogeneous workpiece. For guaranteeing continuity of the deformation as well as equilibrium at the inhomogeneity, suitable compatibility conditions are enforced. Based on such conditions, the thickness of the inhomogeneity can be computed. If this thickness reaches a critical threshold value, localization is assumed to occur.

Model parameter identification

The computation of the parameters defining the constitutive model discussed before is addressed here. For that purpose, an optimization procedure employing a genetic algorithm is adopted (see, e.g., [11], Section 2). Within this algorithm, the objective function defining an error between the experimental measurements obtained from the uni-axial tensile test results presented in [12,6] and the predictions of the model is chosen as

$$\gamma = \sum_{p \in \text{measurements}} \left[\mu_p^{\Sigma}\;\left(\Sigma_p^{\mathrm{set}}/\Sigma_p^{\mathrm{ref}} - 1\right)^2 + \mu_p^{r'}\;\left({r'}_p^{\mathrm{set}}/{r'}_p^{\mathrm{ref}} - 1\right)^2 \right]. \tag{5}$$

Accordingly, the objective function consists of two terms. While the first of those, depending on the stresses $\Sigma_p^{()}$, measures the difference between the experimentally observed and the numerically computed yield loci (also the evolution), the second term is associated with the error in the r-value $r_p'^{()}$ expressed in terms of strain rate ratios. In Eq. 5, μ_p^{Σ} and $\mu_p^{r'}$ are weighting factors. The superscript ref refers to the experimental values, while set refers to the numerically computed values based on a predicted parameter set. For guaranteeing thermodynamical consistence of the resulting model, positive-dissipation is additionally enforced.

The stress responses predicted by the calibrated model is shown in Fig. 1(a). It indicates that the model captures the stress responses in the rolling direction (RD), 45° from RD and the transverse direction (TD) and consequently the planar anisotropy well. Moreover, the strain rate ratios r' in the respective directions plotted in Fig. 1(b) show also an excellent agreement between experiment and the calibrated model.

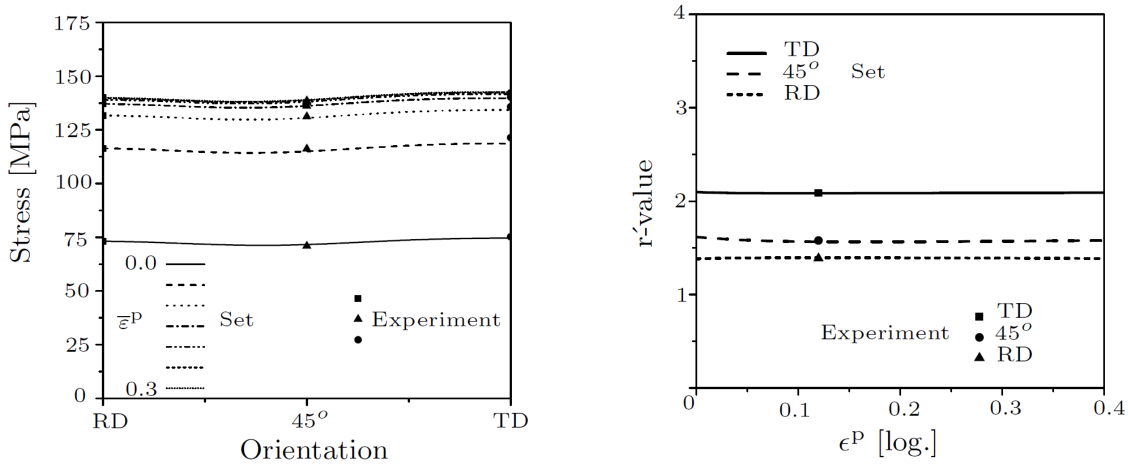

(a) stress responses (b) r-value

Figure 1: Stress responses as a function of material orientation and r'-values as a function of plastic strain: experiment vs. simulation

Application to sheet forming

In this section, the proposed constitutive model is applied for the numerical analysis of sheet forming processes. The experimental setup is fully analogous to that originally used by Nakazima, cf. [18]. As shown in Fig. 2(a), each setup is composed of three tools and a workpiece. The tools are a die, a holder and a punch. In practice the tools undergo a negligible deformation. Therefore, they are assumed to have a rigid structure. By way of contrast, the workpiece is often exposed to a large deformation. Consequently, it has to be described by a suitable constitutive model, e.g., as that discussed within the previous sections. For the complete determination of the forming limit diagram, seven different workpieces are considered; see Fig. 2(b). Within the numerical simulations and in line with experimental observations, the interactions between the tools and the workpiece are controlled by friction.

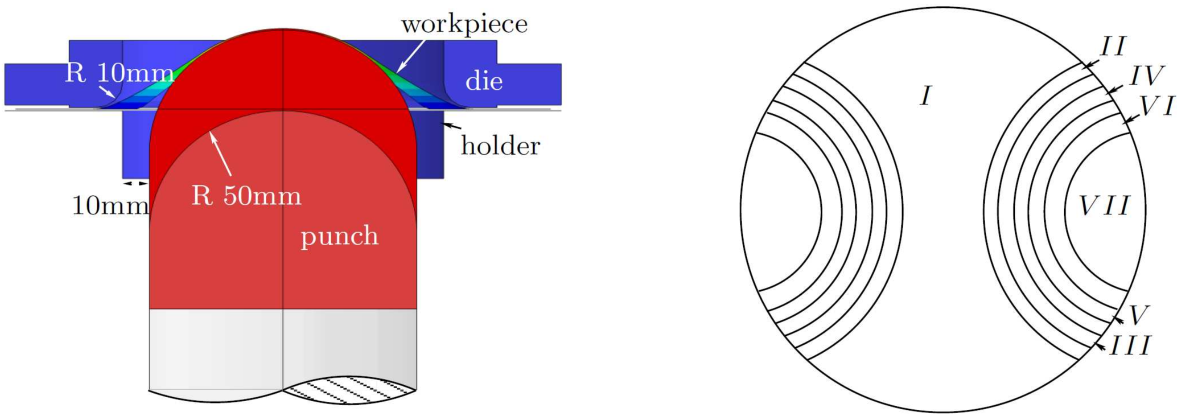

(a) experimental setup (b) workpiece geometries

Figure 2: Experimental setup as proposed by Nakazima (see (18)) and workpiece geometries as modified by Hasek (see (19)) for forming limit test.

The numerically predicted punch displacement vs. punch force diagrams for the different workpieces are shown in Fig. 3. For the sake of comparison, results as computed by means of an isotropic von Mises constitutive model are also depicted. According to Fig. 3(a), the von Mises model underestimates the force response. This may be explained by the higher yield strength recorded in the transverse direction compared to that of the rolling direction. By way of contrast, the novel constitutive model captures the experimental measurements significantly better, see Fig. 3(b). Only for higher deformation levels, the numerical model either underestimates the punch force (geometry I and III), or it overestimates this force (geometry V and VII). At this point, it is assumed that the extrapolation of the mechanical response for non-uniform deformation during the uni-axial tensile tests may have contributed to these discrepancies.

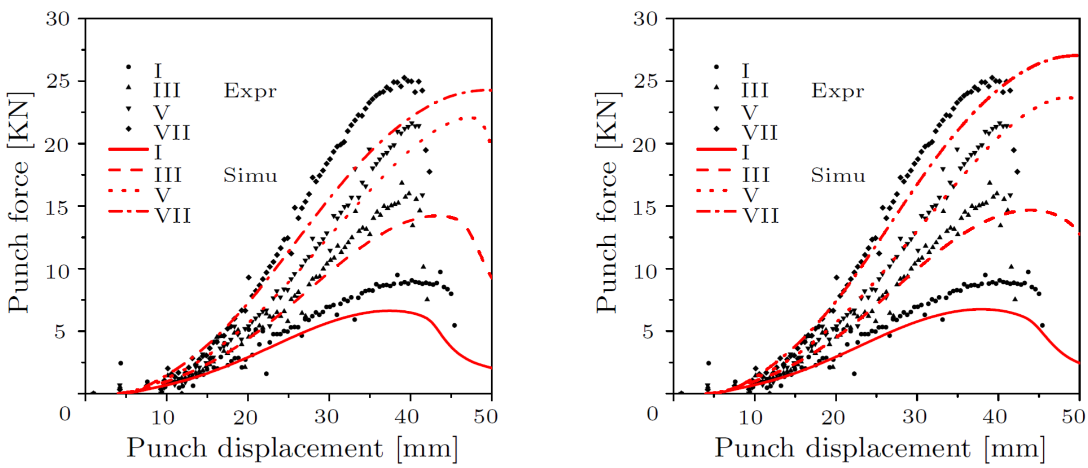

(a) von Mises (b) current model

Figure 3: Forming limit test: comparison of punch force vs. displacement response

Fig. 4(a) shows the strain paths corresponding to the experiments and those related to numerical simulations. Accordingly, except for geometry I, the model predicts the strain paths very well. The numerical prediction of the forming limit strains using the MK localization criterion requires the introduction of a proper geometrical imperfection. For that purpose, simulations with different imperfection magnitudes have been performed. In general, the higher the imperfection the earlier localization occurs. The considered imperfection values, complying with the limit strains reported in [6], range between 2% and 1% of the workpiece thickness.

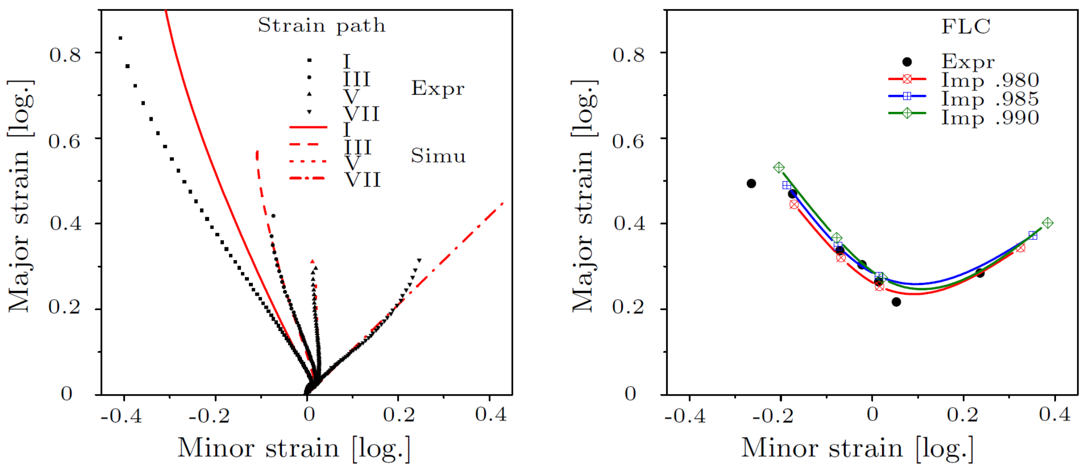

(a) strain path (b) forming limit diagram

Figure 4: Forming limit test: comparison between experimentally and numerically obtained strain paths and forming limits

Conclusion

The proposed thermodynamically consistent constitutive model combined with the MK localization criterion is very promising for numerical analyses of the forming limit response of magnesium at elevated temperatures. Particularly, the developed model captures the experimental observations significantly better than the classical isotropic von Mises model. This is a direct consequence of the more realistic constitutive description, e.g., distortional hardening.

References

[1] E. Kelley, W. Hosford, Transactions of the Metallurgical Scoiety of AIME 242 (1968) 654-661.

[2] J. Bohlen, M. Nurenburg, J. Senn, D. Letzig, S. Agnew, Acta Materialia 55 (2007) 2101-2112.

[3] E. Doege, K. Droeder, Journal of Material Process Technology 117 (2001) 276-281.

[3] E. Doege, K. Droeder, Journal of Material Process Technology 117 (2001) 276-281.

[4] S. R. Agnew, O. Duygulu, Materials Science Forum 419-422 (2003) 177-188.

[5] S. Yi, J. Bohlen, F. Heinemann, D. Letzig, Acta Materialia 58 (2010) 592-605.

[6] M. Nebebe, L. Stutz, J. Bohlen, D. Steglich, D. Letzig, J. Mosler, in: K. Kainer (Ed.), Magnesium-8th International Conference on Magnesium Alloys and their Application, 2009, pp. 764-770.

[7] M. Butuc, Forming limit diagrams. Definition of plastic instability criteria, Ph.D. thesis, Engineering Faculty of Porto University (March 2004).

[8] D. Banabic, H. J. Bunge, K. Poehlandt, A. E. Tekkaya, Springer, 2000.

[9] M. Kuroda, V. Tvergaard, Journal of Solids and Structures 37 (2000) 5037-5059.

[10] Z. Marciniak, K. Kuczynski, Journal of Mechanical Sciences 9 (1967) 609-620.

[11] D. Banabic, Advanced methods in metal forming, Springer, 2007.

[12] M. Nebebe, J. Bohlen, D. Steglich, D. Letzig, International Journal of Material Forming 2 (2009) 53-56.

[13] O. Cazacu, F. Barlat, International Journal of Plasticity 20 (2004) 2027-2045.

[14] G. Cowper, P. Symonds, Tech. Rep. 28, Brown University (1957).

[15] J. Hutchinson, K. Neale, Mechanics of Sheet Metal Forming (1978) 111-126.

[16] J. Hutchinson, K. Neale, Mechanics of Sheet Metal Forming (1978) 127-153.

[17] J. Hutchinson, K. Neale, Mechanics of Sheet Metal Forming (1978) 269-285.

[18] K. Nakazima, T. Kikuma, K. Hasuka, Tech. rep., Yawata (1971).

[19] V. Hasek, Tech. rep., University of Stuttgart (1973).